Proceedings of the International Conference "Underwater Acoustic Measurements: Technologies &Results"
Heraklion, Crete, Greece, 28th June – 1st July 2005

SURFACE WAVES AND FORCED GROUP RESPONSE OBSERVED WITH LRPADS

Jerome A. Smith[a]

[a]Scripps Institution of Oceanography, 9500 Gilman Dr., La Jolla, CA 92093-0213

Dr. J. A. Smith, UCSD mail stop 0213, 9500 Gilman Dr., La Jolla, CA 922093-0213; fax 858-534-7132; email jasmith@ucsd.edu

Abstract: *A novel 32-element Doppler sonar system was deployed to observe waves and currents over a km-scale area of the open ocean. The measurements cover a pie-shaped area about 1.5 km in range by 45 degrees azimuth, with 7.5 m by 1.3 degree resolution. Acoustic sampling every 2.5 seconds over the entire area provides detailed directional wave spectra and simultaneously the response of the underlying flow. The Eulerian response cancels the estimated Stokes drift at the surface, resulting in no net displacement of surface tracers (e.g. bubble clouds) by individual wave groups.*

Keywords: *Surface waves, wave-current interaction, Stokes drift, wave group evolution, Acoustical Oceanography, Underwater Acoustic Measurements*

1. INTRODUCTION

It has long been recognised that waves transport mass and momentum [1, 2]. Both are related to the difference between the average velocity of a fluid parcel (Lagrangian velocity) relative to the current as measured at a fixed point (Eulerian velocity), or "Stokes drift." The vertical integral of the Stokes drift corresponds to both the net mass-flux and the wave momentum per square meter of surface [3]. As waves are strained and refracted by currents, exchanges of mass and momentum occur between the waves and mean flow. In the early 1960's, Longuet-Higgins and Stewart described the "excess flux of momentum due to the presence of waves" and, in analogy to optics, named it the "radiation stress" [3, 4]. Changes in the radiation stress of the waves are compensated for by changes in the mean field, so the overall momentum is conserved. Additional analysis is needed to determine the partitioning

of momentum between waves and the mean. Earlier work [5, 6] provided the basis to describe, for example, the generation of group-bound forced long waves [3, 4].

Surface waves' Stokes drift and the Eulerian response were estimated from a recently gathered oceanic data set. The experiment took place just off the WNW shore of Oahu (Hawaii, USA). An area of the ocean surface roughly 1.5 km radius by 45° in bearing was monitored for velocity and acoustic backscatter intensity, using a novel acoustic Doppler system referred to as the "Long-Range Phased-Array Doppler Sonar" (LRPADS). The area is resolved to 7.5 m in range by 1.3° in bearing (~7000 cells), sampled every 2.5 s, with about 10 cm/s rms error per sample. The vertical aperture encompasses the near-surface bubble layer, which almost always dominates in backscatter intensity over returns from all other depths, and yields a vertical scale-depth for the measurement of about 1.5 m. A sample frame from a sequence of velocity images is shown in figure 1. The three-dimensional (2 space +time) evolution of the surface velocity field can be viewed in the form of movies, or various slices through the 3D data volume or corresponding 3D spectra can be considered.

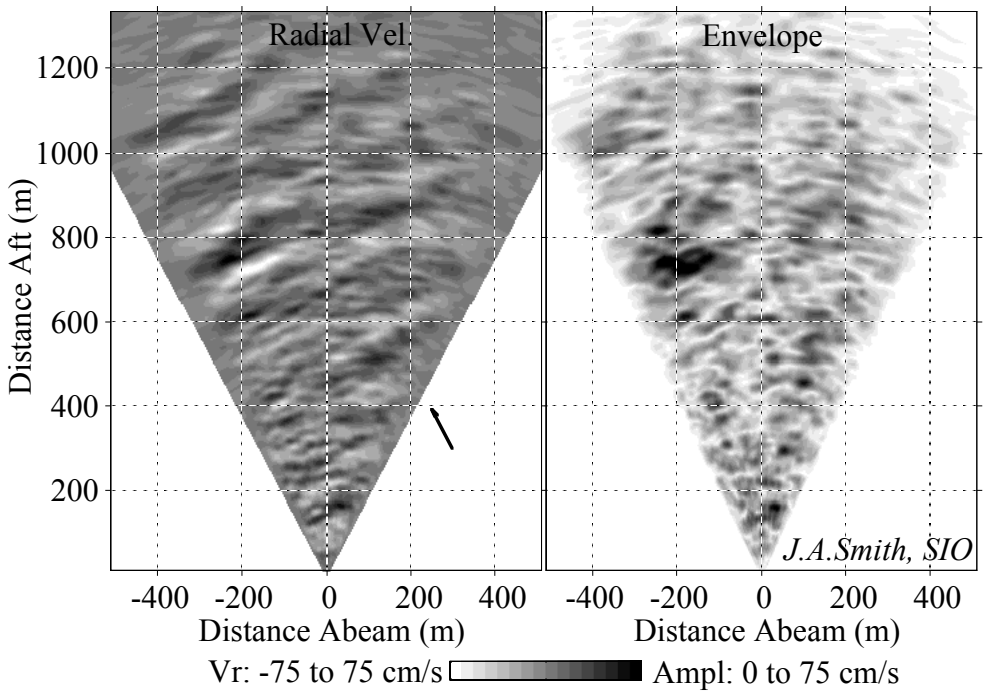

Fig. 1: Example LRPADS image of the surface wave field, showing radial (roughly horizontal) surface orbital velocity component (left panel). The right panel shows the complex amplitude (envelope) of the waves. The black arrow indicates the wind direction and magnitude (near 10 m/s). The waves are propagating roughly downwind.

One way to estimate Stokes drift is to estimate orbital velocities at both a fixed level (Eulerian) and following the surface (semi-Lagrangian: following vertical but not horizontal displacements). In deep water, the difference is just half the Stokes drift (the other half being accounted for by horizontal variations). In the Eulerian frame, counter-flows are observed that cancel the estimated Stokes drift variations at the surface. This is a stronger surface response than expected from the analysis mentioned above. Similar Eulerian counter-flows have been observed in laboratory experiments (e.g., *Klopman* 1994, as referenced in [7]; also [8-12]; and others). The changes in current profile from case to case (no waves, down-current waves, up-current waves) are comparable to the Stokes drift profile calculated from the wave parameters as given (in both magnitude and shape). The observations presented here suggest

that, at least at the surface, the one-to-one balance between the Stokes drift and the induced horizontal Eulerian counter-flow at the surface may be a general result, not confined to the laboratory setting.

2. STOKES DRIFT DUE TO SURFACE WAVES

A wave component introduces horizontal and vertical displacements. Because of the correlated spatial gradients in the wave velocity fields, this introduces a systematic bias in the motion of a fluid particle relative to the average velocity at a fixed point [1]. This relative motion is called the Stokes drift. For a monochromatic small amplitude wave in deep water, the horizontal orbital velocity field can be written as

$$u(x,z,t) = \mathrm{Re}\{U(x,z,t)\} = \mathrm{Re}\{P_u(k,\sigma)e^{kz}\,e^{i(kx-\sigma t)}\} \tag{1}$$

where P_u is a complex velocity amplitude (like a single Fourier component). The horizontal and vertical displacement fields are time integrals of the velocity:

$$\chi = \int_{t_0}^{t} u\,dt = -\sigma^{-1}\,\mathrm{Im}\{U\} \quad \text{and} \quad \zeta = \sigma^{-1}\,\mathrm{Re}\{U\} \tag{2}$$

The velocity gradients are

$$\partial_x u = \mathrm{Re}\{(ik)U\} = -k\,\mathrm{Im}\{U\} \quad \text{and} \quad \partial_z u = \mathrm{Re}\{(k)U\} = k\,\mathrm{Re}\{U\} \tag{3}$$

To second order in wave steepness, the Stokes drift is

$$u^S \approx \{\chi\partial_x u + \zeta\partial_z u\}_{(x,y,t)} = (k/\sigma)\{\mathrm{Im}(U)^2 + \mathrm{Re}(U)^2\} = |U|^2/c \tag{4}$$

Note that half the net Stokes drift comes from the vertical displacements, and half from the horizontal (in deep water).

As an aside, this result is constant with respect to wave phase; i.e., no averaging is required for a monochromatic deep-water wave. However, for a spectrum of waves the nonlinearity of (4) means that shorter waves riding on longer ones introduce high-frequency oscillations to $|U|$, so some form of wave-filtering is required. However, it remains true even for multiple superimposed deep-water waves that half the net Stokes drift comes from vertical and half from horizontal displacements.

3. FREQUENCY-WAVENUMBER SPECTRA

A natural and useful slice through the 3D time-space data volume is a time-range plot, formed along a single direction. Because the heading of FLIP, and hence of the array, can vary by tens of degrees over timescales of minutes, the beamformed data are first interpolated onto a set of fixed directions. Time–range plots reveal both phase propagation and group (envelope) characteristics of surface waves along a given direction. Figure 2 shows a time-range plot for a beam directed roughly downwind. Compact packets of roughly 7 s period waves can be seen, forming slashes at an angle on the time-range plane corresponding to about 5 m/s (the group velocity for 7 s waves, which also have a phase velocity near the

windspeed, 10 m/s). These compact packets are distinct from the spectral peak waves (near 10.6 s), which form broader groups (see Fig. 2).

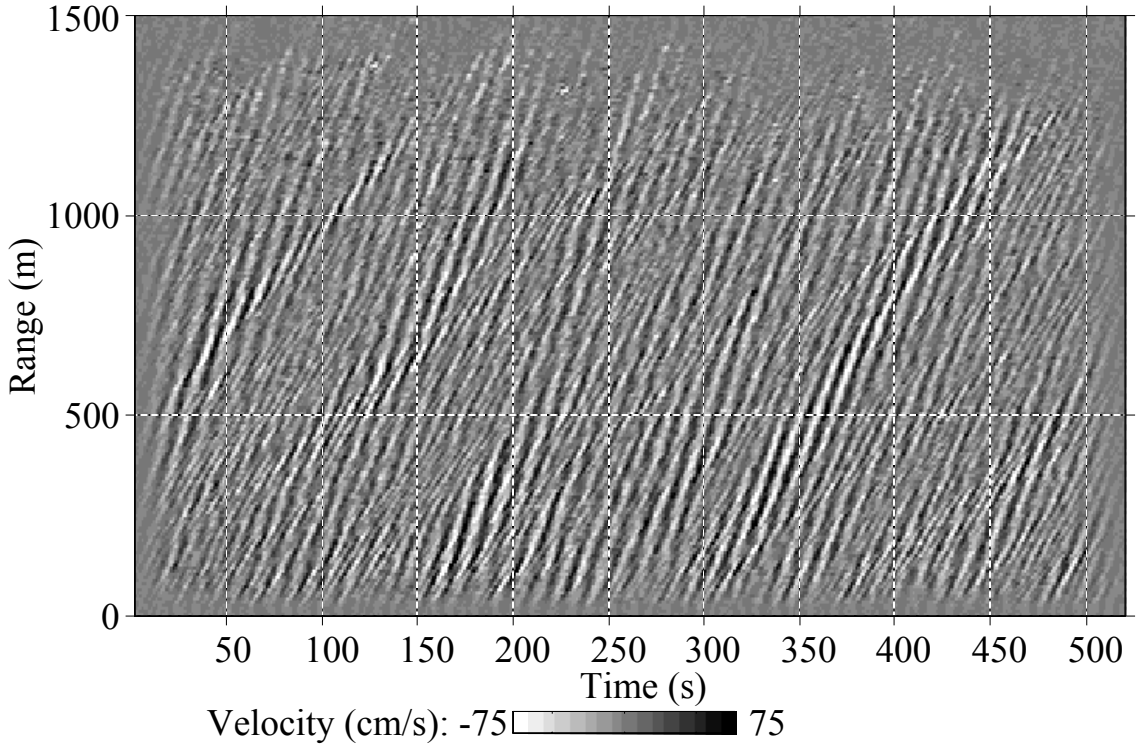

Fig. 2: Time-range plot of radial velocities, dominated by the surface waves' orbital velocity. The highest spectral peak is near 0.1 Hz; note a large wave group starting near 0 m range at 300 s, and moving out to1000 m range by 435 s, corresponding to a group velocity of about 7.5 m/s. Several thinner packets are seen propagating a little slower, at a speed of about 5 m/s. These are compact wave packets, of order one wavelength long (along the vertical axis; i.e. spatially). The frequency associated with these is near 0.14 Hz (7 s period). The corresponding group speed is about 5 m/s, and the phase speed is about equal to the wind speed, 10 m/s.

Figure 3 shows the log-magnitude of the 2D Fourier transform of the data in grey-scale on the *k-f* plane. Since the data are real, the $(+f, +k_r)$ components are redundant with respect to the conjugate $(-f, -k_r)$ components. The wavenumbers are shifted so that $k_r = 0$ is centred; but the frequencies are not shifted, so the aliased variance for frequencies past the Nyquist frequency aligns with the un-aliased variance along the surface wave dispersion curve. The continuity of variance along the dispersion curve suggests this aliased information can be used. Because we know the waves propagate predominantly downwind, the ambiguity of location on the aliased *k-f* plane can be resolved. As seen in figure 3, the resolved (but aliased) surface wave variance extends well past the frequency Nyquist limit, $f_N = 0.2$ Hz, to more than 0.3 Hz. The downwind wave variance can be preserved by cutting these spectra along a diagonal, extending from about (0.08 Hz, -0.065 cpm) to (0.32 Hz, +0.065 cpm). After masking (zero-filling) to remove the redundant information below this line, the otherhalf plane is retained, and the amplitudes are adjusted to preserve the net variance. To resolve the unwrapped wave information, the FFT size is doubled in the *f* direction. The inverse Fourier transform thus has results interpolated to twice the sample rate (samples every 1.25 s rather than 2.5 s). The real part corresponds to the (time-interpolated) original time/space data, and the imaginary part is effectively a Hilbert transform. The complex

magnitude provides useful estimates of the envelope of the motion (useful for the waves and Stokes drift estimation in particular).

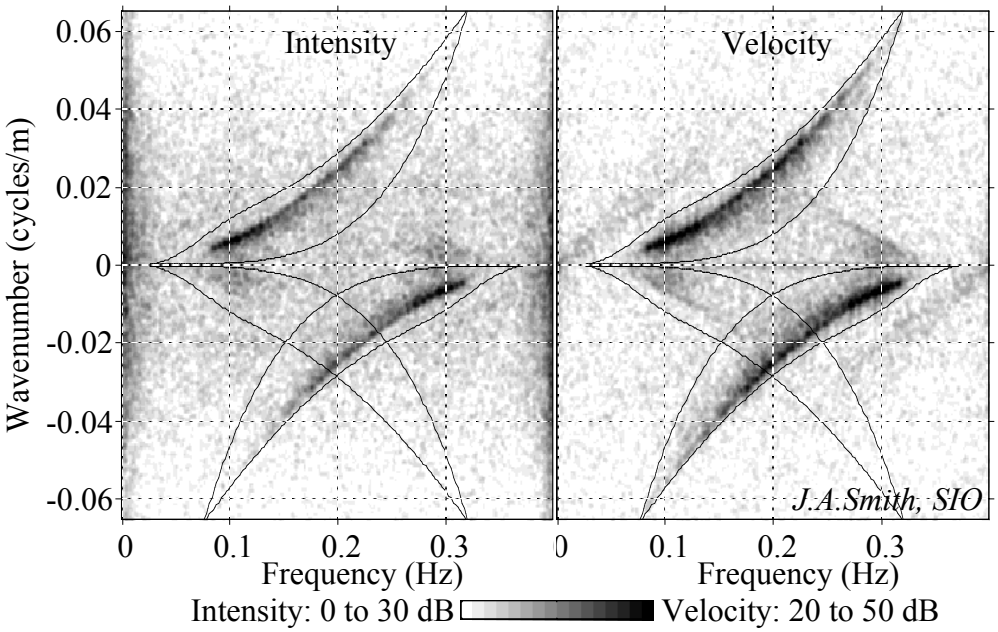

Fig. 3: Wavenumber-frequency spectra from the same time as figure 2. Greyscale represents 10 Log10(variance spectral density, arbitrary units). (Left) spectrum of intensity; (right) spectrum of velocity (roughly horizontal component parallel to beam). The thin lines delimit a separation between "wave-like" and "non-wave" variance in the spectral domain. The surface wave variance continues past the Nyquist frequency (0.2 Hz) in both spectra. The data can be unwrapped by cutting these spectra along a diagonal line favouring downwind propagation. In addition to the surface wave variance (outlined by thin lines), a weaker ridge of variance lies along a line at roughly 45° in the velocity spectrum (but not in intensity), corresponding to propagation at about 5 m/s. This variance is broadly distributed in either k or f alone, so it is difficult to isolate without using both.

One way to estimate the along-beam component of Stokes drift makes use of the vertical displacements alone, yielding exactly half the drift value. The velocity fields are extrapolated vertically from the estimated measurement level to both a constant level (e.g. $z = 0$) and to the moving surface (at $z = \zeta$). Elevation displacements ζ are estimated from the radial component of horizontal velocity, which is unstable for large angles (small k_r). To control this, a smoothly weighted function is employed, using k_{low} (shown in Fig. 3) as a cutoff value (see [13] for details). Since both the radial Stokes drift and sheltering effects are insensitive to the perpendicularly propagating waves, the loss of information is ultimately not important. The estimated elevations are used to explicitly calculate displaced and fixed-level radial velocities, frequency by frequency:

$$u_r^{\zeta}(r,t,f) \approx \{P_u(r,f)e^{-i(2\pi f)t}\}e^{k_f(\zeta - z_m)} \tag{5}$$

$$u_r^{0}(r,t,f) \approx \{P_u(r,f)e^{-i(2\pi f)t}\}e^{-k_f z_m} \tag{6}$$

where z_m is the estimated measurement depth (using straight acoustic rays), and the subscript r denotes the radial (along-beam) component of velocity. The total displacement fields $z_m(r,t)$

and $\zeta(r,t)$ are used for all frequencies. The results are summed over f at each location in range-time space to yield the net displaced (semi-Lagrangian) and fixed-level (Eulerian) radial component of the velocity fields. The wave-averaged difference between the vertically displaced and fixed-level velocities is half the Stokes drift, so the estimate by this method is just twice this. The *k-f* plane separation illustrated in Fig. 3 is used to separate wave-like and non-wave variance. This method has the advantages of explicitly considering the sheltering of crests; properly handling upwind versus downwind directed components; and providing objective estimates of the Eulerian and semi-Lagrangian flows, corrected for sheltering effects. The estimated Stokes drift for the example data segment is shown in Fig. 4.

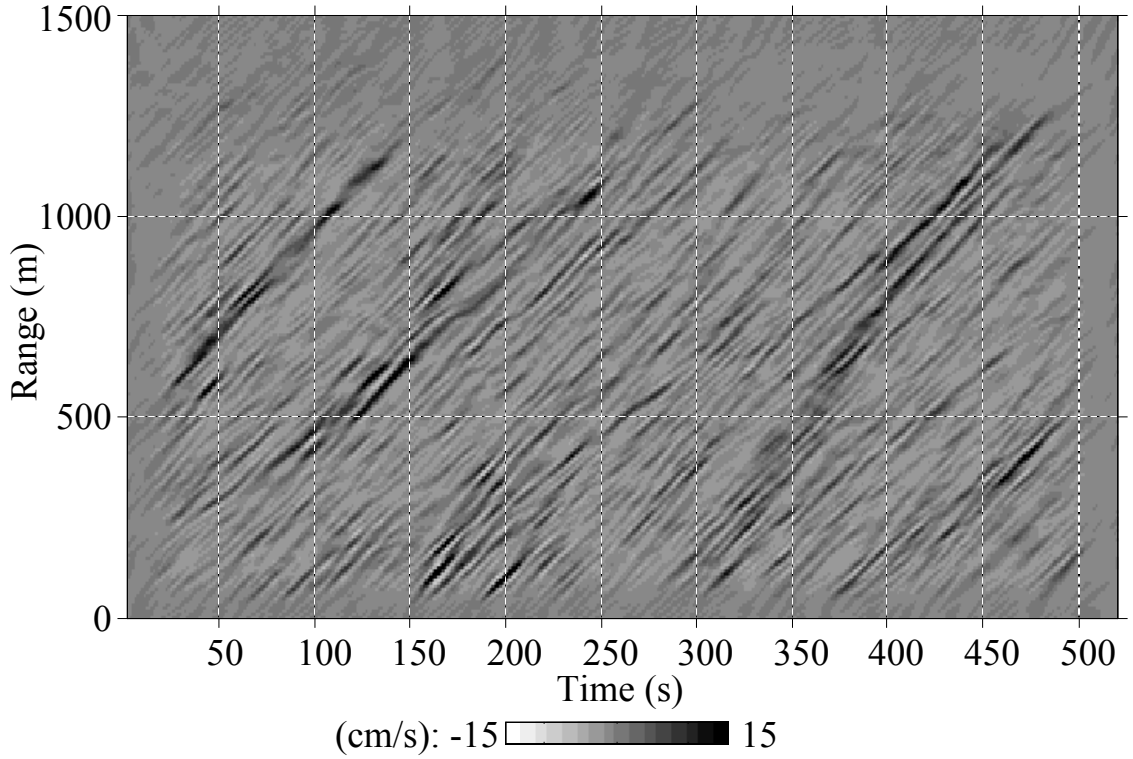

Fig. 4: Time-range plot of the radial Stokes drift for the same segment as in the previous figures (time-means at each range are removed). Note the predominance of slashes at an angle corresponding to roughly 5 m/s propagation along the beam..

The wave-filtered Eulerian velocity field is correlated with the Stokes drift at a statistically significant level. With $N = 208$ samples (the number of pings over which the correlations are averaged), the coherence level for 95% confidence is about 0.12. The measured correlation is several times larger (–0.3 to –0.4) so robust statistical estimates of the transfer function from Stokes drift to the Eulerian anomaly can also be made. The transfer coefficient is about –1.0 at near ranges, increasing slightly with range, indicating that they roughly cancel. Increasing the estimated Stokes drift slightly with range results in complete cancellation. Given the smoothing characteristics of the measurement, such slight underestimation of the Stokes drift is understandable. A linear fit to the transfer coefficient over the range interval 200 – 1000 m was performed, and application of this to the Stokes drift estimates makes them vary less with range (though it still decreases some), without changing the near-range value. This suggests that although measurement sensitivity decreases with range, it still captures the essential characteristics of the Stokes drift. It also suggests that the cancellation of U_S by U_0 is complete.

Adding the estimated Stokes-drift and Eulerian velocities results in an estimate of the fully Lagrangian flow. The *k-f* spectrum of this resulting Lagrangian velocity field shows little evidence of the "5 m/s ridge" (Fig. 5).

The fact that the "5 m/s ridge" disappears from the estimated Lagrangian mean flow is convincing evidence that the Eulerian response is equal and opposite to the Stokes drift (in the near-surface layer sampled). It is difficult to imagine any procedure that could lead coincidentally to such nearly perfect cancellation. Many other data segments have been examined; in every case such cancellation of Stokes drift and Eulerian flow at the surface takes place.

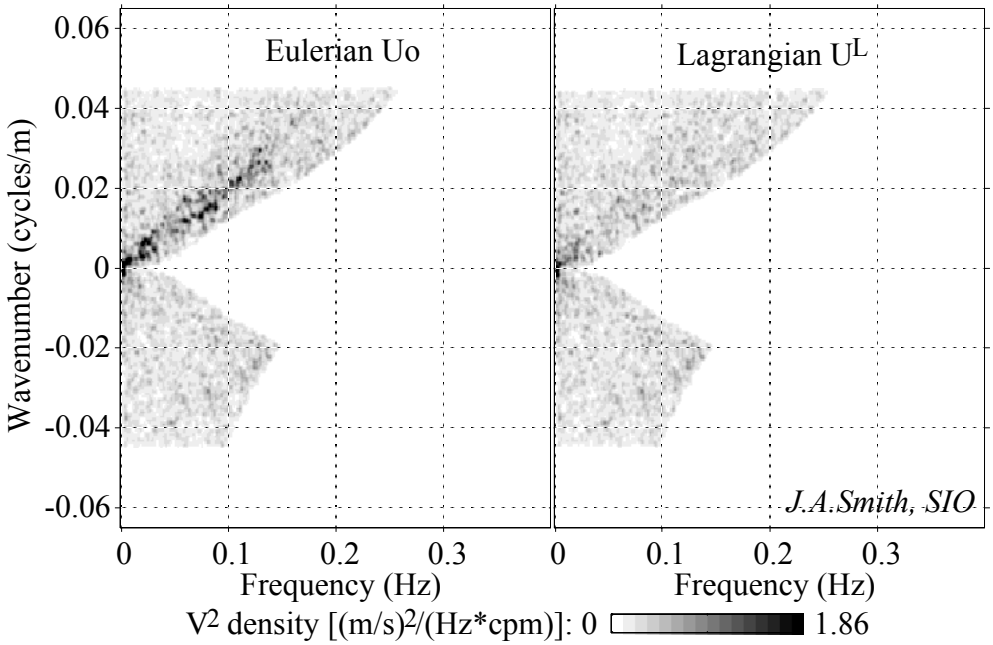

Fig. 5: Wavenumber-frequency spectra for (left) the Eulerian velocity field and (right) the Lagrangian velocity field formed by adding the Eulerian and Stokes drift estimates. The greyscale is linear in variance density, not logarithmic as in Fig. 3. The reduction in variance along the 5 m/s line in the Lagrangian field is dramatic. The remaining variance on the right (U^L) is close to the spectral noise floor.

4. RESULTS

There are two significant scientific results:

1. As wave groups pass, Eulerian counter-flows occur that cancel the Stokes drift variations at the surface.

The magnitude of this counter-flow at the surface exceeds predictions based on an irrotational response [3]; namely, that the response approaches half the surface Stokes drift as the wave group length decreases to a single wave. The mechanism by which this counter-flow is generated is apparently not well understood.

2. The Stokes drift due to open ocean surface waves is highly intermittent.

While this intermittency is expected even with a Rayleigh distribution of wave amplitudes appropriate to random seas [14], the observations also show compact wave "packets" (perhaps too short to be called "groups") that appear to remain coherent for a considerable distance as they propagate. Such coherent packets have not been observed in open ocean deep water conditions previously. As an aside, it may be speculated that since the Eulerian response is of the same order as finite amplitude dispersion corrections, it may be important in understanding wave group dynamics.

5. ACKNOWLEDGEMENTS

This work was supported by the ONR Physical Oceanography program (C/G# N00014-90-J-1285). I thank J. Klymak, R. R. Guza, Pinkel, K. Melville, J. Polton, and many others for useful discussions and suggestions. A big thanks also to the OPG engineering team of E. Slater, M. Goldin, and M. Bui for their tireless efforts to design, construct, deploy, and operate the LRPADS, and in helping to develop the software to analyse the resulting data..

REFERENCES

[1] **G. G. Stokes**, On the theory of oscillatory waves, *Trans. Camb. Phil. Soc.*, 8, pp. 441-455, 1847.
[2] **M. S. Longuet-Higgins**, Mass transport in water waves, *Phil. Trans.*, A 245, pp. 535-581, 1953.
[3] **M. S. Longuet-Higgins and R. W. Stewart**, Radiation stress and mass transport in gravity waves, with application to 'surf-beats', *J. Fluid Mech.*, 13, pp. 481-504, 1962.
[4] **M. S. Longuet-Higgins and R. W. Stewart**, Radiation stress in water waves; a physical discussion, with applications, *Deep Sea Res.*, 11, pp. 529-562, 1964.
[5] **M. S. Longuet-Higgins and R. W. Stewart**, Changes in the form of short gravity waves on long waves and tidal currents, *J. Fluid Mech.*, 8, pp. 565-583, 1960.
[6] **M. S. Longuet-Higgins and R. W. Stewart**, Short gravity waves on steady non-uniform currents, *J. Fluid Mech.*, 10, pp. 529, 1961.
[7] **J. Groeneweg and G. Klopman**, Changes of the Mean Velocity Profiles in the Combined Wave-Current Motion Described in a GLM Formulation, *Journal of Fluid Mechanics*, 370, pp. 271-296, 1998.
[8] **P. H. Kemp and R. R. Simons**, The interaction of waves and a turbulent current; waves propagating against the current, *J. Fluid Mech.*, 130, pp. 73-89, 1983.
[9] **P. H. Kemp and R. R. Simons**, The interaction of waves and a turbulent current; waves propagating with the current, *J. Fluid Mech.*, 116, pp. 227-250, 1982.
[10] **C. Swan**, Convection within an experimental wave flume, *J. Hydraul. Res.*, 28, pp. 273-282, 1990.
[11] **J.-Y. Jiang and R. L. Street**, Modulated flows beneath wind-ruffled, mechanically generated water waves, *J. Geophys. Res. (Oceans)*, 98 (C2), pp. 2711-2721, 1991.
[12] **S. G. Monismith, E. A. Cowen, H. M. Nepf, J. Magnaudet, and L. Thais**, Mean flows under surface gravity waves, *(unpublished manuscript)*, 1996.
[13] **J. A. Smith**, Observed Variability of Ocean Wave Stokes Drift, and the Eulerian Response to Passing Groups, *J. Phys. Oceanogr.*, submitted, preprint at http://jerry.ucsd.edu/JSmith_PDF/Waves&StokesDrift_050.pdf, pp. 42, 2005.
[14] **M. S. Longuet-Higgins**, On wave breaking and the equilibrium spectrum of wind generated waves, *Proc. Roy. Soc.*, A311, pp. 371-389, 1969.